IL NUOVO CIMENTO VOL. 2 A, N. 2 21 Marzo 1971

Multiperipheral Dynamics and Inclusive Experiments (*).

D. SILVERMAN and C.-I TAN

Joseph Henry Laboratories, Princeton University - Princeton, N. J.

(riceveto il 4 Agosto 1970)

Summary. — The relationship between multiperipheral dynamics and inclusive experiments at high energy is developed. The general features of the single-particle distribution spectrum are exhibited for multiperipheral models with exponential damping in the momentum transfers. By working with a specific multi-Regge model we further demonstrate the phenomena of pionization and of scaling in longitudinal momentum for small momentum transfers. Examples of distribution spectra are given for specific and physically important values of Regge parameters. The predictions can serve as a test for a realistic model for the integral-equation approach to multiperipheral dynamics, and can provide a sensible form for parametrizing experimental data.

1. – Introduction.

The progress of the Regge model of high-energy scattering has been fruitfully stimulated by close interactions with experiments. The current theoretical development in multiperipheral dynamics [1] and multi-Regge bootstrap mo-

(*) Research Sponsored by the Air Force Office of Scientific Research under Contract AF 49 (638)-1545.

(1) L. BERTOCCHI, S. FUBINI and M. TONIN: *Nuovo Cimento*, **25**, 626 (1962); D. AMATI, A. STANGHELLINI and S. FUBINI: *Nuovo Cimento*, **26**, 896 (1962) (hereafter ABFST), and references therein. Recently CHEW *et al.* (Lawrence Radiation Laboratory preprint UCRL-19457) have argued forcefully that the ABFST model, with a properly guessed off-shell $\pi\pi$ elastic cross-section, has a firmer physical basis than the multi-Regge bootstrap models. Nevertheless, they further noted that if one forgoes the requirement

dels ([2,3]) may also benefit from consideration of the uniquely related inclusive experiments, *e.g.* the single-particle production spectrum ([4-6]). We concern ourselves in this paper with developing this relation. We show how the single-particle spectrum is given in a general multiperipheral model. Then, using a simplified multi-Regge bootstrap model of an internal Regge coupling which is exponentially damped in momentum transfer ([4]), we derive explicit expressions for the single-particle momentum distribution at high energy. We discuss in detail the phenomena of pionization ([1]), large-transverse-momentum damping, and small-momentum-transfer particle production, all of which emerge from the multiperipheral model in a natural way. The predictions can be compared with experiments ([4,6]), and serve as tests of a realistic model for the integral-equation approach to multiperipheral production. They also provide understanding of the general structure of high-energy production processes, and provide a sensible form for parametrizing experimental data.

The main feature of multiperipheral dynamics is the incorporation of direct-channel unitarity with the factorizable multiperipheral approximation to production amplitudes. The multiperipheral integral equation has been developed to compute the contribution of all multiparticle intermediate states to the elastic absorptive part. This same method can be used for any inclusive production experiment, in which a specific set of final particles is measured, and the cross-section summed over all other particles which may be produced ([5]). The simplest examples of an inclusive experiment are the total cross-section and the single-particle distribution spectrum, where only one final particle is measured. The production of the undetected particles can be summed over by the integral-equation approach, and the spectrum of an inclusive experi-

---

of a « direct » bootstrap cycle, multi-Regge models can be so interpreted as to include the ABFST model as a special case. Since our treatment does not require detailed knowledge of bootstrap mechanisms, and we are not restricting ourselves only to pion production, these different interpretations of multiperipheralism do not concern us here.

([2]) G. F. CHEW, M. L. GOLDBERGER and F. LOW: *Phys. Rev. Lett.*, **22**, 208 (1969) (hereafter referred to as CGL); G. F. CHEW and C. DE TAR: *Phys. Rev.*, **180**, 1577 (1969); M. CIAFALONI, C. DE TAR and M. N. MISHELOFF: *Phys. Rev.*, **183**, 2522 (1969); L. CANESCHI and A. PIGNOTTI: *Phys. Rev.*, **180**, 1525 (1969); **184**, 1915 (1969); G. F. CHEW and W. R. FRAZER: *Phys. Rev.*, **181**, 1914 (1969); J. S. BALL and G. MARCHESINI: *Phys. Rev.*, **188**, 2209, 2508 (1969); A. H. MUELLER and I. J. MUZINICH: *Ann. of Phys.*, (to be published); Brookhaven Report No. BNL-13836 (unpublished); I. G. HALLIDAY and L. M. SAUNDERS: *Nuovo Cimento*, **60** A, 177 (1969); M. L. GOLDBERGER: *Erice Summer School, 1969* (unpublished).

([3]) M. L. GOLDBERGER, C.-I TAN and J. M. WANG: *Phys. Rev.*, **184**, 1920 (1969); D. SILVERMAN and C.-I TAN: *Phys. Rev. D*, **1**, 3479 (1970); S. PINSKY and W. I. WEISBERGER: Princeton report (to be published).

([4]) L. CANESCHI and A. PIGNOTTI: *Phys. Rev. Lett.*, **22**, 1219 (1969).

([5]) R. P. FEYNMAN: *Phys. Rev. Lett.*, **23**, 1415 (1969).

([6]) D. SILVERMAN and C.-I TAN: *Phys. Rev. D*, **2**, 233 (1970).

ment can be expressed in terms of the solution of the integral equation associated with the elastic absorptive part. Thus the analysis of inclusive experiments can be used as a test of the methods of the integral-equation approach. On the other hand, this application of the multiperipheral integral equation will help us to understand the behaviour of inclusive experiments and provide a parametric representation which may be used to fit the data.

In this paper we analyse the single-particle spectrum to achieve a more detailed analysis of the features of the multi-Regge integral equation than can be obtained from studying the total cross-section or the multiplicity of produced particles. We concentrate on the process where the observed particle arises from a central position on a multiperipheral chain, which accounts for most of the single-particle spectrum. The process of emission from the end of the chain, which was covered in a previous paper ([6]), accounts for only the very forward or backward production, but it is also important since it can be more directly expressed in terms of the solution of the multi-Regge integral equation. We examine what is basically the same model that was applied by CANESCHI and PIGNOTTI ([4]) to calculate numerically fits to single-particle distribution data. In view of the close relation of the single-particle distribution to the multi-Regge bootstrap model, we realize the importance of calculating the results of the model in analytic form in order to understand the characteristic features of the spectrum and the explicit dependence on the parameters. By treating the phase-space Jacobian exactly, we obtain a different formulation of the single-particle distribution spectrum from that of CANESCHI and PIGNOTTI ([4]).

The calculation of the single-particle spectrum for the central emission from a multipheral chain begins by writing the multi-Regge production amplitude for a chain with a cluster of particles on each side of the observed particle. The single-particle cross-section is computed by squaring the amplitude, integrating over the phase space of all but the observed particle, and then summing over the number of particles in each cluster from one to infinity. In this procedure we ignore all crossed graphs for conventional reasons. The sum over the number of particles in a cluster is the same process used in deriving the integral equation for the elastic absorptive part, and the contribution of this sum may be expressed in terms of the solution of the multi-Regge integral equation. To get the single-particle spectrum as a function of the momentum components of the observed particle, we must then integrate the resulting form over the momentum transfers connecting the clusters to the observed particle t_l, t_r, and over the total energies of the clusters s'_l, s'_r.

We then proceed to calculate the single-particle spectrum with a concrete model which has Regge behaviour in the cluster energies and exponential damping in the multiperipheral momentum transfers. The integrals over the momentum transfers are then done exactly. We can then establish general features of the single-particle spectrum and do the integrals over the sub-

energies for the special but important cases where the intercepts of the exchanged trajectories are 0 or $\frac{1}{2}$. These results are then simplified in certain kinematic regions to give some illustrations of the form of the single-particle spectrum.

The results of our investigation can be grouped into those of a general nature and those that follow from the specific multi-Regge assumptions. The general multiperipheral assumption of exponential damping in momentum transfer of the internal Regge coupling is shown to lead to exponential damping of the cross-section in $q_\perp^2$, and to a natural classification of regions of single-particle phase space. The general assumption also leads to the existence of regions where the majority of physical events take place, *i.e.* the pionization region where momentum $|\boldsymbol{q}|$ is small in the c.m. frame, and the forward- and backward-production regions. The more specific assumptions of the damped multi-Regge model and its bootstrap results allow us to obtain definite results for the distribution spectrum. Assuming the intercept of the bootstrapped Pomeranchuk trajectory to be unity, the spectrum is shown to possess the property of pionization ([1]) in the region of small momentum in the c.m. frame, and the scaling property in longitudinal momentum ([7]) in the forward- and backward-production regions. It also indicates the dominance of the end diagrams in the small M^2 areas of the forward- and backward-production regions. For illustrative purposes, we exhibit simplified spectra for special values of the Regge parameters in a way which allows the parametrization of the experiments in the various kinematic regions.

In Sect. **2** we review various integral-equation approaches to the multi-Regge bootstrap model, and then relate these approaches to the single-particle distribution spectrum. Using the results of the exponentially damped multi-Regge model, we proceed in Sect. **3** to express the central-diagram contribution to the spectrum as a double integral over the total energies of the clusters. We do this integration analytically for special values of the Regge-trajectory intercepts. In Sect. **4**, we discuss the general features of the spectrum as well as the specific consequences of the multi-Regge model. A summary of our investigation is presented in Sect. **5**.

2. – Multi-Regge bootstrap model and single-particle distribution spectrum.

We first briefly review the integral-equation formulation of the multi-Regge bootstrap model. We shall discuss both the formulation of CHEW, GOLDBERGER and LOW ([2]), and the simplified Reggeon-particle absorptive-am-

([7]) S. DRELL: *Proceedings of Madison Conference on High-Energy Physics* (1970); H. PIOTROWSKA: *Phys. Lett.*, **32** B, 71 (1970).

plitude approach ([3]). We then relate these integral equations to the single-particle distribution spectrum.

2·1. *Review of multi-Regge bootstrap model.* – The multi-Regge bootstrap model employs unitarity to calculate the n-particle intermediate-state contribution A_n to the forward elastic absorptive part A in terms of the n-particle production amplitude T_n:

$$A = \sum_{n=1}^{\infty} A_n = \tfrac{1}{2} \sum_n \int \mathrm{d}\Phi^n |T_n|^2 \,. \tag{2.1}$$

By using a factorizable multi-Regge exchange approximation to T_n in which the contribution of each final particle is factorizable, we may write a recursion relation and integral equation for an amplitude related to A.

For simplicity we shall consider a multi-Regge model for a spinless scalar particle. This production amplitude T_n for a 2 to n process is approximated in the multi-Regge region by the product form

$$T_n = G_l H_{n-1} \beta_{n-1} H_{n-2} \beta_{n-2} \ldots \beta_2 H_1 G_r \,, \tag{2.2}$$

and is a function of the invariants $\Sigma_j \equiv (q_{j+1} + q_j)^2$, $t_j \equiv \left(k - \sum_{i=1}^{j} q_i\right)^2$, and the Toller angles ω_j (see Fig. 1). $G_l(t_{n-1})$ and $G_r(t_1)$ are single Regge couplings and $\{\beta_j(t_j, \omega_j, t_{j-1})\}$ are double Regge couplings. The Regge factor $H_j(t_j, \Sigma_j)$ is given by $\xi(t_j) \cdot (\Sigma_j/\mu^2)^{\alpha(t_j)}$, where $\alpha(t_j)$ is the Regge trajectory and $\xi(t_j)$ contains the signature factor and physical poles, and is normalized to have unit residue at $t_j = \mu^2$.

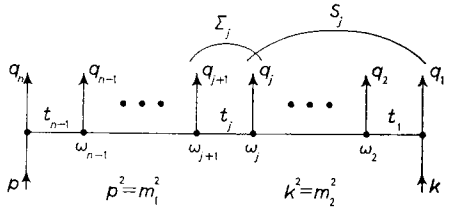

Fig. 1. – Kinematics of the multi-Regge chain.

One can also express the amplitude T_n in terms of $\{t_i\}$, $\{\omega_j\}$, and invariant energies $s_k \equiv \left(\sum_{i=1}^{k} q_i\right)^2$, $k = 1, \ldots, n$. In the multi-Regge region of large s_j and Σ_j,

([8]) F. ZACHARIASEN and G. ZWEIG: *Phys. Rev.*, **160**, 1322 (1967).

strong ordering ([8]), *i.e.* $s_{j+1} \gg s_j$, results in the following kinematic relation:

$$\Sigma_j = \frac{s_{j+1}}{s_j} f(t_j, \omega_j, t_{j-1}) , \tag{2.3}$$

where

$$f(t_j, \omega_j, t_{j-1}) = \frac{\Delta(t_j, \mu^2, t_{j-1})}{\mu^2 - t_j - t_{j-1} + 2\sqrt{t_j t_{j-1}} \cos\omega_j} \tag{2.4}$$

with

$$\Delta(x, y, z) = x^2 + y^2 + z^2 - 2xy - 2yz - 2zx .$$

We can thus replace the Regge factor $H_j(t_j, \Sigma_j)$ by

$$\xi(t_j)\left[\frac{f(t_j, \omega_j, t_{j-1})}{\mu^2}\right]^{\alpha(t_j)} \left(\frac{s_{j+1}}{s_j}\right)^{\alpha(t_j)}$$

in eq. (2.2). This replacement can be thought of as a different, though equally plausible, multiperipheral approximation from that of eq. (2.2). They are equivalent to each other in the multi-Regge region, and the validity of their extrapolations to the low-energy region are equally speculative. For simplicity, we will use the latter multiperipheral approximation.

In this formulation, the physical two-body forward absorptive amplitude $A(p, k)$ can be expressed in terms of a Reggeon-particle absorptive amplitude $\mathscr{A}(p', k)$, which satisfies a linear integral equation ([3]). The relation between $A(p, k)$ and $\mathscr{A}(p', k)$ is

$$A(p, k) = A_1(p, k) + \int \frac{\mathrm{d}^4 p'}{(2\pi)^3} \delta^+((p - p')^2 - \mu^2) |G_i(t')|^2 |\xi(t')|^2 \left(\frac{s}{s'}\right)^{2\alpha(t')} \mathscr{A}(p', k), \tag{2.5}$$

where $A_1(p, k) = \pi |G_r(\mu^2)|^2 \delta^+(s - \mu^2)$ is the single-particle contribution. The integral equation for $\mathscr{A}$ computes the sum of all n-particle intermediate-state multi-Regge ladder diagrams, as shown in Fig. 2. (One can also show that on

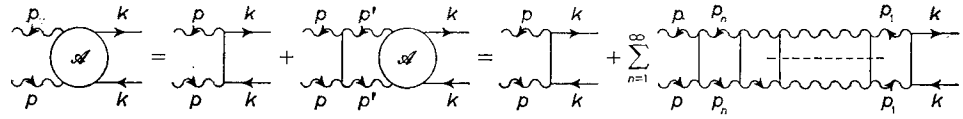

Fig. 2. – The integral equation for the Reggeon-particle absorptive part as the sum of all multi-Regge ladder diagrams.

the mass shell $A(p, k) = \mathscr{A}(p, k)$, $p^2 = \mu^2$, thus justifying our naming $\mathscr{A}(p', k)$ the Reggeon-particle absorptive amplitude.) This simplified integral equation has been studied extensively ([3]). At large $s' = (p' + k)^2$, $\mathscr{A}(p', k)$ has been shown

to possess Regge behavior

$$\mathscr{A}(p', k) \equiv \mathscr{A}(p'^2; (p'+k)^2) \propto \left(\frac{(p'+k)^2}{\mu^2}\right)^{\alpha_{\text{out}}(0)}, \tag{2.6}$$

where $\alpha_{\text{out}}(0)$ is the intercept of the dynamical output Regge pole of the model.

The CGL approach requires the introduction of an auxiliary function $B(p, p'; k)$, which satisfies the CGL integral equation ([2]), and is related to $A^{\text{CGL}}(p, k)$ by

$$A^{\text{CGL}}(p, k) = A_1(p, k) + \int \frac{\mathrm{d}^4 p'}{(2\pi)^3} \delta^+((p-p')^2 - \mu^2) |G_i(t')|^2 B(p, p'; k) . \tag{2.7}$$

In the limit of strong ordering, these two formulations become equivalent, and B is then related to $\mathscr{A}$ by

$$B(p, p'; k) = \left(\frac{(p+k)^2}{(p'+k)^2}\right)^{2\alpha(t')} \mathscr{A}(p', k) . \tag{2.8}$$

2·2. *Relation of single-particle distribution spectrum to multi-Regge bootstrap model.* – The single-particle distribution spectrum is the differential cross-section measured by a scattering experiment at a fixed energy which only detects one particle in the final state to have four-momentum q^μ and thereby sums over all other particles which are produced. In the multi-Regge picture outlined above, the detected particle may arise from either an end or a more central position on a multiperipheral chain, as shown in the diagrams in Fig. 3.

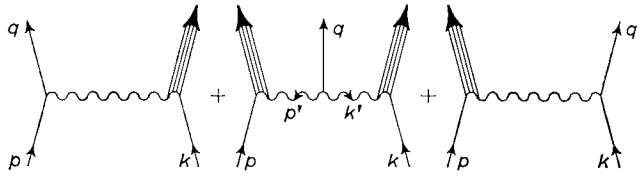

Fig. 3. – The left-end, central and right-end contributions to the single-particle distribution spectrum.

To obtain the single-particle distribution cross-section $\mathrm{d}\sigma/\mathrm{d}^3\boldsymbol{q}$ we add the multi-Regge amplitude T_n for the diagrams of n produced particles, eq. (2.2), square, and integrate over phase space, and then sum over n. Using the conventional method of dropping cross-terms, we end up with a sum of ladder diagrams (see Fig. 7) which may be related to the sum forming the multi-Regge integral equation for $\mathscr{A}$ (Fig. 2). The details of this procedure are carried out in Appendix A. The resulting single-particle distribution spectrum is then given

in terms of the solution to the integral equation for B or $\mathscr{A}$ by (see Fig. 4)

$$(2.9)\qquad \frac{\mathrm{d}\sigma}{\mathrm{d}^4q\,\delta^+(q^2-\mu^2)} = \frac{1}{(2\pi)^3\Delta^{\frac{1}{2}}(s, m_1^2, m_2^2)}\Big\{G_i^2((p-q)^2)\,B(p, p-q; k) + \\ + \frac{2}{(2\pi)^4}\int \mathrm{d}^4p'\,\mathrm{d}^4k'\,\delta^4(p'+k'+q)\,B(-k', p'; p)|\beta(p'^2, \omega, k'^2)|^2\,B(-p', k'; k) + \\ + G_r^2((k-q)^2)\,B(k, k-q; p)\Big\}.$$

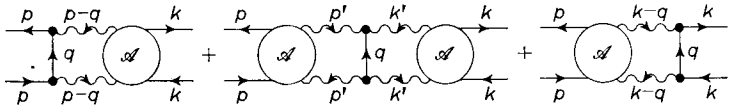

Fig. 4. – Relation of the single-particle distribution to the integral-equation amplitude.

The first and last terms are the contributions of the end diagrams in Fig. 3 and are derived and discussed in an earlier paper ([6]). The middle term is the contribution of the central diagram, the study of which in a simple model is the primary concern of this paper.

3. – Single-particle spectrum from a simple multi-Regge model.

To proceed to understand the single-particle distribution spectrum from the multi-Regge bootstrap model we calculate the spectrum using a simple model for the Regge residue and the related solution of the integral equation for $\mathscr{A}$.

3·1. *The exponentially damped multi-Regge model.* – The basis of the model is that strong-interaction amplitudes decrease rapidly when any momentum transfer becomes large. Experiments indicate that this decrease in momentum transfer is approximately exponential, and our simple model for the internal Regge vertex is

$$(3.1)\qquad \beta(t_j, \omega_j, t_{j-1}) \simeq \frac{G(t_j)G(t_{j-1})}{g}, \qquad G(t) = g\exp[\Omega(t-\mu^2)].$$

For rapid damping in momentum transfer, the main contribution to the cross-section will come from small momentum transfer where the approximate ω-angle independence of the coupling has been indicated by TAN and WANG ([9]). Under this approximation of rapid damping, the integral equation for $\mathscr{A}(t; s)$ in this

([9]) C.-I TAN and J. M. WANG: *Phys. Rev.*, **185**, 1988 (1969).

model has a separable kernel, and the solution has Regge behavior and exponential damping in (mass)^2 of the Reggeon

$$\mathscr{A}(t;s) \simeq \frac{G(t)^2}{g^2} s^{\alpha(0)} . \tag{3.2}$$

The results of this model for the contributions of the end diagrams have been discussed in a previous paper ([6]). We now apply this model to the contribution from the central diagram.

The kinematical notation for the central diagram is given in Fig. 5. Using the relations eqs. (2.8) and (3.2) and considering the overall magnitude to

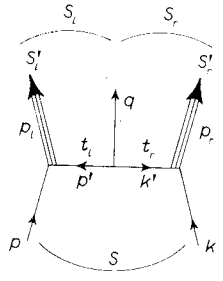

Fig. 5. – The central diagram, $p^2 = m_1^2$, $k^2 = m_2^2$, $q^2 = \mu^2$.

be an adjustable parameter we have from eq. (2.9) the central-diagram contribution of this model:

$$\frac{\mathrm{d}\sigma}{\mathrm{d}^4 q\, \delta^+(q^2-\mu^2)} = \frac{\lambda}{s}\int\!\!\int \mathrm{d}^4p'\, \mathrm{d}^4k'\, \delta^4(p'+k'+q)(s'_l)^{\alpha_p(0)}\left(\frac{s_l}{s'_l}\right)^{2\alpha_l(t_l)}(\exp[\Omega'_l t_l])\cdot \tag{3.3}$$

$$\cdot(\exp[\Omega'_r t_r])\left(\frac{s_r}{s'_r}\right)^{2\alpha_r(t_r)}(s'_r)^{\alpha_p(0)}.$$

The absorptive parts are assumed to be Pomeranchuk dominated, and $\alpha_l(t_l)$ and $\alpha_r(t_r)$ are the trajectories carrying the momentum transfers t_l and t_r in Fig. 5. We assume these trajectories to be linear:

$$\alpha_l(t_l) = \alpha_l + \alpha'_l t_l\,, \qquad \alpha_r(t_r) = \alpha_r + \alpha'_r t_r\,. \tag{3.4}$$

The model is the same as that used by CANESCHI and PIGNOTTI ([4]). The essential differences in our treatment will be to do the integrals analytically rather than numerically, and to exhibit general features and simple specific results of the model.

3·2. *Multiperipheral phase-space integration over momentum transfers.* – In order to perform the integration in eq. (3.3), we convert to invariant variable

integrations. The single detected final-state particle has two independent momentum components in the c.m. system, the longitudinal component $q_{\parallel}$ and the magnitude of the perpendicular component $q_{\perp}$. Of the three invariants formed from the particle momentum q,

$$M^2 \equiv (p+k-q)^2\,, \qquad u_l \equiv (p-q)^2\,, \qquad u_r \equiv (k-q)^2\,, \tag{3.5}$$

we may consider any pair to be independent variables since they are related by

$$s = M^2 - u_l - u_r + m_1^2 + m_2^2 + \mu^2\,. \tag{3.6}$$

The physical variables we are interested in integrating over are the cluster energies s_l', s_r', and the momentum transfers t_l, t_r. The remaining variables s_l, s_r are now dependent variables:

$$s_l = s_l' - u_l - t_l + t_r + m_1^2 + \mu^2\,, \qquad s_l = s_r' - u_r - t_r + t_l + m_2^2 + \mu^2\,. \tag{3.7}$$

The Jacobian for this change of variables is

$$\iint \mathrm{d}^4p'\,\mathrm{d}^4k'\,\delta^4(p'+k'+q) = \iint \mathrm{d}s_l'\,\mathrm{d}s_r' \int \frac{\mathrm{d}t_l\,\mathrm{d}t_r}{16\sqrt{-\Delta_4}}\,\theta(-\Delta_4)\,, \tag{3.8}$$

where

$$\Delta_4 = \begin{vmatrix} p_l^2 & p_l\cdot p_r & p_l\cdot p & p_l\cdot k \\ p_r\cdot p_l & p_r^2 & p_r\cdot p & p_r\cdot k \\ p\cdot p_l & p\cdot p_r & p^2 & p\cdot k \\ k\cdot p_l & k\cdot p_r & k\cdot p & k^2 \end{vmatrix}. \tag{3.9}$$

The physical region for the production process is given by

$$\Delta_4 \leqslant 0\,.$$

In terms of the invariant variables

$$\Delta_4 = \begin{vmatrix} s_l' & \tfrac{1}{2}(M^2-s_l'-s_r') & \tfrac{1}{2}(-t_l+s_l'+m_1^2) & \tfrac{1}{2}(M^2-u_l+t_r-s_r') \\ \tfrac{1}{2}(M^2-s_l'-s_r') & s_r' & \tfrac{1}{2}(M^2-u_r+t_l-s_l') & \tfrac{1}{2}(-t_r+m_2^2+s_r') \\ \tfrac{1}{2}(-t_l+s_l'+m_1^2) & \tfrac{1}{2}(M^2-u_r+t_l-s_l') & m_1^2 & \tfrac{1}{2}(M^2-u_l-u_r+\mu^2) \\ \tfrac{1}{2}(M^2-u_l+t_r-s_r') & \tfrac{1}{2}(-t_r+m_2^2+s_r') & \tfrac{1}{2}(M^2-u_l-u_r+\mu^2) & m_2^2 \end{vmatrix}$$

In order to do the t_l, t_r integrations in a simple form we take advantage of the strong damping in t_l, t_r to neglect the contributions of t_l, t_r to s_l, s_r (eqs. (3.7)), and approximate

$$s_l \simeq s_l' - u_l\,, \qquad s_r \simeq s_r' - u_r\,, \tag{3.10}$$

in the dynamical Regge forms $(s_l/s_l')^{2\alpha_l(t_l)}$ and $(s_r/s_r')^{2\alpha_r(t_r)}$, but not in the Jacobian. The single-particle distribution spectrum is then a sum over all contributing trajectories with the form

$$\frac{\mathrm{d}\sigma}{\mathrm{d}^4q\,\delta^+(q^2-\mu^2)} = \sum_{\alpha_l,\alpha_r} \lambda_{\alpha_l\alpha_r} \Phi_{\alpha_l\alpha_r}\,,$$

$$\Phi_{\alpha_l\alpha_r} = \frac{1}{16s}\iint \mathrm{d}s_l'\,\mathrm{d}s_r'(s_l')^{\alpha_p(0)}\left(\frac{s_l'-u_l}{s_l'}\right)^{2\alpha_l(0)}\left(\frac{s_r'-\mu_r}{s_r'}\right)^{2\alpha_r(0)}(s_r')^{\alpha_p(0)}\,I(s_l', s_r')\,, \tag{3.11}$$

where $I(s_l', s_r')$ represents the integral over $\mathrm{d}t_l$, $\mathrm{d}t_r$:

$$I(s_l', s_r') = \iint \frac{\mathrm{d}t_l\,\mathrm{d}t_r}{\sqrt{-\Delta_4}}\,\theta(-\Delta_4)\exp[\Omega_l t_l + \Omega_r t_r] \tag{3.12}$$

and

$$\begin{cases} \Omega_l = \Omega_l' + 2\alpha_l' \ln\left(\dfrac{s_l'-u_l}{s_l'}\right), \\ \Omega_r = \Omega_r' + 2\alpha_r' \ln\left(\dfrac{s_r'-u_r}{s_r'}\right). \end{cases} \tag{3.13}$$

An integral of the same form as $I(s_l', s_r')$ has been performed by CHAN *et al.* ([10]), in the Appendix to their paper. If we compare our work with their formula (A.2) we find the mathematical problem to be the same under the following mapping of their variables to our variables ([11]):

	CHAN *et al.*'s *notation*	*Our notation*
(3.14)	$(m_1^2, m_2^2, m_3^2, m_4^2, m_5^2)$,	$(s_l', s_r', m_1^2, \mu^2, m_2^2)$,
	$(s, s_{34}, s_{45}, t_{13}, t_{25})$,	$(M^2, u_l, u_r, t_l, t_r)$.

([10]) CHAN HONG-MO, K. KAJANTIE and G. RANFT: *Nuovo Cimento*, **49** A, 157 (1967).

([11]) One cannot directly use the results of CHAN *et al.*, because their physical situation holds for s_l, s_r, s_l', s_r' fixed, whereas the single-particle distribution has u_l and u_r fixed with the other variables constrained only by eqs. (3.7).

The result of their eqs. (A.4), (A.5) and (37) gives us

$$I(s_l', s_r') = 4\pi \exp[-b] \exp[a_l(s_l'/M^2) + a_r(s_r'/M^2)] \cdot \cdot \left\{ \frac{\sinh [c\Delta^{\frac{1}{2}}(1, s_l'/M^2, s_r'/M^2)]}{c} \right\}, \tag{3.15}$$

where

$$\begin{cases} b = \Omega_l(M^2 - u_r - m_1^2) + \Omega_r(M^2 - u_l - m_2^2), \\ a_l = \Omega_l(M^2 + u_r - m_1^2) + \Omega_r(M^2 - u_l + m_2^2), \\ a_r = \Omega_l(M^2 - u_r + m_1^2) + \Omega_r(M^2 + u_l - m_2^2), \\ c = \{\Omega_l^2 \Delta(M^2, u_r, m_1^2) + \Omega_r^2 \Delta(M^2, u_l, m_2^2) + \\ \quad + 2\Omega_l \Omega_r [M^2(M^2 - u_l - u_r - m_1^2 - m_2^2 + 2\mu^2) - (u_l - m_2^2)(u_r - m_1^2)]\}^{\frac{1}{2}}. \end{cases} \tag{3.16}$$

Since we have treated the Jacobian exactly, our result for the momentum transfer integrations differs from that of ref. [4].

3·3. *Integration over cluster energies.* – In order to perform the integrals over s_l', s_r' in a tractable form, we restrict ourselves to the cases where the intercepts of the exchanged trajectories α_l, α_r are equal to 0 or $\frac{1}{2}$. They would correspond to physical exchange of the pion or rho trajectory, or trajectories degenerate with these. If one wishes to fit data using α_l, α_r as parameters, one may numerically perform the s_l', s_r' integrations in eq. (3.11). We also make the approximation of neglecting the terms with s_l' and s_r' dependence in Ω_l and Ω_r, eq. (3.13), since at present accelerator energies it is experimentally known that diffraction peaks are mainly due to exponential damping of the residues, or $\Omega_l' \gg 2\alpha_l'$, $\Omega_r' \gg 2\alpha_r'$. We note that now the coefficients c, b, a_l, a_r depend only on the invariants fixed by the single-particle momentum, and not on s_l', s_r'.

In the integral eq. (3.11), using the result eq. (3.15), we make the simplifying change of variables

$$\frac{s_l'}{M^2} = z(1-x), \qquad \frac{s_r'}{M^2} = x(1-z). \tag{3.17}$$

The boundary of the integration region is given by

$$\Delta^{\frac{1}{2}}\left(1, \frac{s_l'}{M^2}, \frac{s_r'}{M^2}\right) = 1 - x - z = 0, \tag{3.18}$$

and the Jacobian is

$$\mathrm{d}s_l' \mathrm{d}s_r' = (M^2)^2(1-x-z)\,\mathrm{d}x\,\mathrm{d}z.$$

We then split the integral into two terms by writing

$$(3.19)\quad \sinh\left[c\Delta^{\frac{1}{2}}\left(1, \frac{s_l'}{M^2}, \frac{s_r'}{M^2}\right)\right] = \frac{1}{2}[\exp[c(1-x-z)] - \exp[-c(1-x-z)]] .$$

By making the substitution in the second term $z = 1 - x'$ and $x = 1 - z'$, its integrand becomes identical to the first term, and joining them gives the result

$$(3.20)\quad \Phi_{\alpha_l\alpha_r} = \frac{\pi}{8}\frac{(M^2)^2}{sc}\exp[-b]\int_0^1 dx \int_0^1 dz(1-x-z)\cdot$$
$$\cdot\exp[a_l z(1-x) + a_r x(1-z) + c(1-x-z)]\, \mathscr{I}_{\alpha_l\alpha_r}(x, z) ,$$

where the Regge power terms give

$$(3.21)\quad \mathscr{I}_{\alpha_l\alpha_r}(x, z) =$$
$$= (M^2)^{2\alpha_p}[z(1-x) + \tau_l]^{2\alpha_l}[z(1-x)]^{\alpha_p - 2\alpha_l}[x(1-z) + \tau_r]^{2\alpha_r}[x(1-z)]^{\alpha_p - 2\alpha_r} ,$$

and

$$(3.22)\qquad \tau_l \equiv -\frac{u_l}{M^2}, \qquad \tau_r \equiv -\frac{u_r}{M^2} .$$

For the restricted case of α_l, α_r equal to 0 or $\frac{1}{2}$ we have, with $\alpha_p = 1$,

$$(3.23)\qquad \mathscr{I}_{\alpha_l\alpha_r}(x, z) = (M^2)^2[z(1-x) + \tau_l\delta_{\alpha_l,\frac{1}{2}}][x(1-z) + \tau_r\delta_{\alpha_r,\frac{1}{2}}] .$$

These polynomial terms may be removed from the integrand by formal differentiation of the exponent with respect to a_l, a_r, or c. The result of the integration for these restricted cases, α_l and α_r equal to 0 or $\frac{1}{2}$, is then finally

$$(3.24)\quad \Phi_{\alpha_l\alpha_r} = \frac{\pi}{8}\frac{(M^2)^4}{sc}\left(\frac{d}{da_l} + \tau_l\delta_{\alpha_l,\frac{1}{2}}\right)\left(\frac{d}{da_r} + \tau_r\delta_{\alpha_r,\frac{1}{2}}\right)\left(\frac{d}{dc}\right)\cdot\left(\frac{1}{a_l + a_r}\right)\cdot$$
$$\cdot\left\{\exp[-b-c]\left[\exp\left[\frac{(c+a_l)(c+a_r)}{a_l+a_r}E_1\left(\frac{(c+a_l)(c+a_r)}{a_l+a_r}\right)\right]\right] -\right.$$
$$-\exp[-b+a_l]\left[\exp\left[\frac{(c+a_l)(c-a_l)}{a_l+a_r}E_1\left(\frac{(c+a_l)(c-a_l)}{a_l+a_r}\right)\right]\right] -$$
$$-\exp[-b+a_r]\left[\exp\left[\frac{(c+a_r)(c-a_r)}{a_l+a_r}E_1\left(\frac{(c+a_r)(c-a_r)}{a_l+a_r}\right)\right]\right] +$$
$$\left. + \exp[-b+c]\left[\exp\left[\frac{(c-a_l)(c-a_r)}{a_l+a_r}E_1\left(\frac{(c-a_l)(c-a_r)}{a_l+a_r}\right)\right]\right]\right\} ,$$

where $E_1(x)$ is the exponential function.

The regions of importance of the separate terms, and their expressions in certain simple kinematic limits will be discussed in the next Section. The form above could also be used for computer evaluation.

4. – General and specific results of the model.

We begin by pointing out general features of the multiperipheral single-particle spectrum which should apply to more general models and are illustrated by eq. (3.24). These general features are results of the multiperipheral assumption that the production amplitudes are strongly damped in the momentum transfers, and they are relatively independent of the power-law behavior in the subenergies, such as Regge behavior. In the latter part of this Section we present specific results of the exponentially damped multi-Regge model in various kinematic regions.

4·1. *General features of multiperipheral single-particle spectra.* – The kinematic region of the detected particle in the c.m. momenta $q_\parallel$, $q_\perp$ is shown in Fig. 6, where for s large the boundary is a semi-circle of radius $q_{\max} \simeq q^0_{\max} \simeq \sqrt{s}/2$.

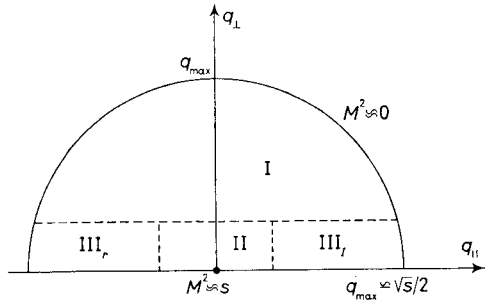

Fig. 6. – Single-particle phase space in the c.m. frame.

(Our convention is $p_\parallel = -k_\parallel \geqslant 0$.) For the purposes of this Subsection, we approximate the kinematics for large s and drop masses where feasible. The invariants become

$$\text{(4.1)} \qquad \begin{cases} -u_l \simeq \sqrt{s}(q_0 - q_\parallel)\,, \\ -u_r \simeq \sqrt{s}(q_0 + q_\parallel)\,, \\ M^2 \simeq s(1 - q_0/q^0_{\max})\,, \\ \dfrac{u_l u_r}{s} \simeq \mu^2 + q_\perp^2\,, \end{cases}$$

where

$$q_0 = \sqrt{q_\perp^2 + q_\parallel^2 + \mu^2}\,.$$

The main feature of eq. (3.24) is the exponential decrease of the terms as given by the exponents

$$
(4.2)\quad \begin{cases} -b + a_l \simeq 2\Omega_l u_r\,, \\ -b + a_r \simeq 2\Omega_r u_l\,, \\ -b + c \simeq -\Omega_l(M^2 - u_r) - \Omega_r(M^2 - u_l) + \\ \qquad + \sqrt{[\Omega_l(M^2 - u_r) + \Omega_r(M^2 - u_l)]^2 - 4\Omega_l\Omega_r u_l u_r}\,, \\ \text{and} \\ -b - c < -b + c\,. \end{cases}
$$

This exponential behavior is a consequence of the assumed multiperipheral exponential behavior in momentum transfers and is independent of the power behavior of the subenergies as generated by the derivatives in eq. (3.24). We may include the end diagrams in this discussion by noting that u_l and u_r are the momentum transfers for the left- and right-end diagrams, respectively. In the exponentially damped model of eqs. (3.1) and (3.2), the cross-sections from the end diagrams are found to have exponential residues with exponents

$$\text{left end: } 2\Omega_l u_l\,, \qquad \text{right end: } 2\Omega_r u_r.$$

The exponential damping generally occurs in the variable $q_\perp^2$: examination of eqs. (4.1) and (4.2) for $q_\parallel \gg \sqrt{\mu^2 + q_\perp^2}$ and with $\Omega_l = \Omega_r = \Omega/2$ gives for the least damped terms

$$
\begin{aligned}
-b + a_l &\simeq -\Omega\,\frac{q_{\max}}{q_\parallel}(q_\perp^2 + \mu^2)\,, \\
-b + c &\simeq -\frac{\Omega}{1 - q_\parallel/2q_{\max}}(q_\perp^2 + \mu^2)\,.
\end{aligned}
$$

In analysing the general features we have found that the single-particle phase space has a natural division into four kinematic regions, which are indicated in Fig. 6. The cross-sections in the various regions receive contributions from different ranges of the subenergies s_l' and s_r'. These may be found by examining the coefficients in the exponent in eq. (3.20) and the relation of the x, z variables to s_l' and s_r', eqs. (3.17). The definitions of the four regions and the properties of the cross-section in each region are given below.

1) *Large-transverse-momentum region*: $q_\perp = O(\sqrt{s})$; $u_l, u_r = O(s)$. The cross-section is exponentially damped with exponent of order $(-s)$. The contributing subenergies are $s_l', s_r' = O((\text{mass})^2)$. The dominant exponential term in eq. (3.24) is

$$-b + c = -s\Omega\left\{\left(1 - \frac{q_0}{2q_{\max}}\right) - \sqrt{\left(1 - \frac{q_0}{2q_{\max}}\right)^2 - \frac{q_\perp^2 + \mu^2}{4q_{\max}^2}}\right\},$$

where for simplicity we have set $\Omega_l = \Omega_r = \Omega/2$.

2) *Pionization region*: $q = O(\text{mass})$, $q_\parallel = O(\text{mass})$; $u_l, u_r = O(\sqrt{s})$. The cross-section is independent of $q_\parallel$ and s. The contributing subenergies are s_l', $s_r' \leqslant O(\sqrt{s})$. The dominant exponential term is

$$-b + c = -\frac{2\Omega_l \Omega_r}{\Omega_l + \Omega_r} q_\perp^2 .$$

3*a*) *Forward-production region*: $q_\perp = O(\text{mass})$, $q_\parallel = O(\sqrt{s})$ and positive; $u_l = O((\text{mass})^2)$, $u_r = O(s)$. The dominant exponential terms are $-b + c$, $-b + a_l$, and the left-end diagram, all of which are of order $\Omega(\text{mass})^2$. The contributing subenergies are $s_l' = O((\text{mass})^2)$, $s_r' \leqslant M^2 = O(s)$.

3*b*) *Backward-production region*: $q_\perp = O(\text{mass})$, $q_\parallel = O(\sqrt{s})$ and negative; $u_r = O((\text{mass})^2)$, $u_l = O(s)$. The dominant exponential terms are $-b + c$, $-b + a_r$, and the right-end diagram, all of which are of order $\Omega(\text{mass})^2$. The contributing subenergies are $s_r' = O((\text{mass})^2)$, $s_l' \leqslant M^2 = O(s)$.

From the above analysis we find that the end diagrams are only important in the forward- or backward-production regions. We also observe that in the large-momentum-transfer region the cross-section is severely damped by exponents of order s, whereas the cross-section is not greatly damped in the regions with small $q_\perp$. In regard to the form used for the behavior in the subenergies, we find that the pionization region is most sensitive to the assumptions at high subenergies, the large-momentum-transfer region to the form at low subenergies, and the forward- and backward-production regions are dependent on both.

4·2. *Some simple results of the exponentially damped multi-Regge model.* – We shall now concentrate on specific features of the single-particle spectrum of the exponentially damped multi-Regge model. We discuss the phenomena of pionization, scaling in longitudinal momentum, and damping at large q^2. We also exhibit, for illustration, the functional forms of the spectrum in the four general regions of phase space, under simplified assumptions. These predictions can easily be used to compare with and parametrize experimental data.

1) *Large-transverse-momentum region.* This region is characterized by $|q_\perp| = O(\sqrt{s})$. In this limit, only the term associated with the factor $\exp[-b + c]$ in eq. (3.24) contributes substantially, and all relevant combinations of parameters, *i.e.* $c - a_l$, $c - a_r$, $a_l + a_r$ and $b - c$, are of order s (eq. (3.16)). Instead of actually carrying out the formal differentiation in eq. (3.24), we find that in this region $\Phi_{\alpha_l, \alpha_r}$ can be obtained for general values of α_r and α_l by working with eq. (3.20) directly. Writing the exponential term in the integrand as

$$\exp[-(c - a_r)x - (c - a_l)z - (a_l + a_r)xz + c], \tag{4.3}$$

we observe that the only region in the x-z plane where the integrand will contribute significantly is restricted to $0 \leqslant x, z \leqslant O(1/s)$. We can thus drop the term $-(a_r + a_l)xz$, keep only the zeroth-order term in the rest of the integrand, and extend the integration limits to ∞. The remaining double integral can easily be done and yields

$$\Phi_{\alpha_l \alpha_r} \simeq \left[\frac{\pi}{32} \frac{(M^2)^2}{(\Omega_l + \Omega_r)^2} \frac{[\tau_l(a_l - c)]^{2\alpha_l}[\tau_r(a_r - c)]^{2\alpha_r}}{sc(b-c)^2} \cdot \right. \\ \left. \cdot \Gamma(2-2\alpha_l)\,\Gamma(2-2\alpha_r)\right] \exp[-(b-c)]\,. \tag{4.4}$$

These various combinations of a_r, a_l, b and c in this limit can be obtained from eq. (3.16), and, in the simple case $\Omega_l = \Omega_r = \Omega/2$ and for $|q_\perp|/|q_\perp|_{\max} < 1$, they become

$$\begin{cases} a_r = \Omega s\left(1 - \dfrac{q_0}{q_{\max}} + \dfrac{q_\parallel}{2q_{\max}}\right), \\ a_l = \Omega s\left(1 - \dfrac{q_0}{q_{\max}} - \dfrac{q_\parallel}{2q_{\max}}\right), \\ b = \Omega s\left(1 - \dfrac{q_0}{2q_{\max}}\right), \\ c = \Omega s \sqrt{\left(1 - \dfrac{q_0}{2q_{\max}}\right)^2 - \dfrac{q_\perp^2}{4q_{\max}^2}}\,. \end{cases} \tag{4.5}$$

2) *Pionization region.* This region is characterized by $|\boldsymbol{q}|^2 = O((\text{mass})^2)$ in the c.m., or u_l, $u_r = O(\sqrt{s})$, $M^2 = s$. We shall first work with eq. (3.20) to demonstrate the general phenomenon of pionization [12], *i.e.* the single-particle distribution spectrum is independent of s and $q_\parallel$ in this region. We shall next restrict ourselves to the cases α_r, $\alpha_l = 0$ or $\frac{1}{2}$, and obtain explicit functional forms for the spectrum.

The coefficients of x, z and xz in eq. (4.3) are given in this region by

$$\begin{cases} -(c - a_l) \simeq 2\Omega_l u_r \simeq -2\Omega_l \sqrt{s}\,(q_0 + q_\parallel)\,, \\ -(c - a_r) \simeq 2\Omega_r u_l \simeq -2\Omega_r \sqrt{s}\,(q_0 - q_\parallel)\,, \\ -(a_l + a_r) \simeq -2(\Omega_l + \Omega_r)s\,. \end{cases} \tag{4.6}$$

Since the dominant contribution comes from the region $0 \leqslant x$, $z \leqslant O(1/\sqrt{s})$, we can again keep only the zeroth-order term in the rest of the integrand, and

---

[12] The term « pionization » is used here, for pedagogical reasons, to describe this special phenomenon, and applies to the production of all hadrons. It is not restricted only to pions.

extend the integration limits to ∞. That is, we can approximate the Regge term as

$$\mathscr{I}_{\alpha_l\alpha_r} \simeq s^{2\alpha_p}[z+\tau_l]^{2\alpha_l}[z]^{\alpha_p-2\alpha_l}[x+\tau_r]^{2\alpha_r}[x]^{\alpha_p-2\alpha_r},$$

where α_p will be set to unity and $\tau_l \simeq -u_l/s$, $\tau_r \simeq -u_r/s$. If we now scale x, z by $x' = (-u_l)x$, $z' = (-u_r)z$ and use the properties in this region, $u_l u_r \simeq s(\mu^2 + q_\perp^2)$, $c \simeq s(\Omega_l + \Omega_r)$, and

$$-b + c \simeq -\frac{2\Omega_l\Omega_r}{\Omega_l+\Omega_r} q_\perp^2, \tag{4.7}$$

we obtain

$$\Phi_{\alpha_l\alpha_r} \simeq s^{\alpha_p-1}\Phi'_{\alpha_l\alpha_r},$$

where $\Phi'_{\alpha_l\alpha_r}$ is a function of $q_\perp^2$ only. Setting $\alpha_p = 1$, we find that the resulting cross-section, eq. (3.11), is independent of s and $q_\parallel$ in this region.

This property of pionization has been noted by ABFST ([1,13]) in their study of the original multiperipheral model. We have here an explicit demonstration of this property in the context of the multi-Regge model.

For the actual functional form of $\Phi_{\alpha_l\alpha_r}$, we consider eq. (3.24), where α_l, α_r are restricted to be 0 or $\frac{1}{2}$. The dominant term is again that associated with the factor $\exp[-b+c]$. Carrying out the formal differentiation, we obtain in this region

$$\Phi_{\alpha_l\alpha_r} = \frac{\pi}{32}\frac{1}{\Omega_l+\Omega_r} C_{\alpha_l\alpha_r}(\tau)\exp\left[-\frac{2\Omega_l\Omega_r}{\Omega_l+\Omega_r}\cdot q_\perp^2\right],$$

where

$$C_{0,0} = (1+\tau)\,e^\tau E_1(\tau) - 1,$$

$$C_{0,\frac{1}{2}} = e^\tau E_1(\tau) + \frac{\Omega_r}{\Omega_l}(1-\tau e^\tau E_1(\tau)),$$

$$C_{\frac{1}{2},0} = e^\tau E_1(\tau) + \frac{\Omega_l}{\Omega_r}(1-\tau e^\tau E_1(\tau)),$$

$$C_{\frac{1}{2},\frac{1}{2}} = (1+\tau)\,e^\tau E_1(\tau) - 1 + \frac{(\Omega_l+\Omega_r)^2}{\Omega_l\Omega_r},$$

and

$$\tau \equiv \frac{(a_l-c)(a_r-c)}{a_l+a_r} \simeq \frac{2\Omega_l\Omega_r}{\Omega_l+\Omega_r}(q_\perp^2+\mu^2). \tag{4.8}$$

([13]) Results of ABFST have also been summarized and discussed by D. Tow: *Some predictions of the* ABFST *multiperipheral models*, to be published in *Phys. Rev.*

Since $(e^{\tau}E_1(\tau)-1)\sim 1/\tau$ has a smooth dependence on $q_\perp^2$, the factor $\exp[-b+c]$, which in this limit behaves as

$$\exp\left[-\frac{2\Omega_l\Omega_r}{\Omega_l+\Omega_r}q_\perp^2\right],$$

provides a sharp fall off in $q_\perp^2$ to the cross-section. Furthermore, since the term controlling the pionization region in eq. (3.24) is the same one that controls the large-transverse-momentum region, this terms exhibits the continuity of the $q_\perp^2$ dependence through both of the regions.

3) *Forward- and backward-production region.* We will work in the forward-production region characterized by $|q_\perp|^2=O((\text{mass})^2)$, $q_\parallel\simeq q_0=O(\sqrt{s})$ and positive, so that $u_l=O((\text{mass}^2))$. The results for the backward region are directly obtained by the interchange $u_l\leftrightarrow u_r$, $\Omega_l\leftrightarrow\Omega_r$, $m_1^2\leftrightarrow m_2^2$, and the change of the sign of $q_\parallel$ to negative. We shall first demonstrate that the single-particle distribution cross-section scales in the longitudinal momentum, that is, it depends on $q_\parallel$ and s only in the form $(q_\parallel/q_{\max})$, where $q_{\max}=\sqrt{s}/2$. This behavior of the experimental data has been pointed out by DRELL [7]. Further, it has the approximate behavior in $q_\perp^2$ of

$$\frac{\mathrm{d}\sigma}{\mathrm{d}^4q\,\delta^+(q^2-\mu^2)}=\exp[-\nu q_\perp^2]f\left(\frac{q_\parallel}{q_{\max}}\right);$$

ν will depend on $(q_\parallel/q_{\max})$ smoothly. We shall next exhibit the functional form of $\Phi_{\alpha_l\alpha_r}$ for the special case at $q_\perp^2=0$, and $\mu^2=m_1^2=m_\pi^2$. Lastly, we discuss the behavior of $\Phi_{\alpha_l\alpha_r}$ as $(M^2/s)\to 0$, and examine the relative importance of end diagrams *vs.* central diagrams for the extreme forward limit as well as for the general limit of $|\boldsymbol{q}|\to q_{\max}$.

The dependence on $(q_\parallel/q_{\max})$ is expressed in the variable

$$\beta\equiv\frac{M^2}{s}\simeq 1-q_0/q_{\max}\simeq 1-\frac{q_\parallel}{q_{\max}}.$$

The coefficients of x, z and xz in the exponential term of eq. (4.3) are given in this region by

$$-(c-a_l)\simeq 2\Omega_l u_r=-2\Omega_l s(1-\beta),$$

$$-(c-a_r)\simeq -2\beta\frac{[\Omega_l(\Omega_l+\Omega_r)m_1^2+\Omega_r(\Omega_l+\Omega_r)u_l-\Omega_l\Omega_r\mu^2]}{\Omega_l+\beta\Omega_r},$$

$$-(a_l+a_r)=-2(\Omega_l M^2+\Omega_r M^2)=-2(\Omega_l+\Omega_r)\beta s,$$

where

$$u_l\simeq m_1^2\beta-\frac{\beta\mu^2+q_\perp^2}{1-\beta}. \tag{4.9}$$

We immediately note that the only region of importance in the z integration is $0 \leqslant z \leqslant O(1/s)$. We can thus keep only the zeroth-order approximation in z in the rest of the integrand, and then relax the integration region to $(0, \infty)$, *i.e.* approximate

$$\mathscr{I}_{\alpha_l,\alpha_r} = s^{2\alpha_p}\beta^{2\alpha_p}[z(1-x)+\tau_l]^{2\alpha_l}[z(1-x)]^{\alpha_p-2\alpha_l}[x+\tau_r]^{2\alpha_r}[x]^{\alpha_p-2\alpha_r},$$

where

$$\tau_l \equiv -\frac{u_l}{M^2} \simeq \frac{1}{\beta s}\left(\frac{q_\perp^2+\beta\mu^2}{1-\beta}-\beta m_1^2\right),$$

$$\tau_r \equiv -\frac{u_r}{M^2} \simeq \frac{1-\beta}{\beta}.$$

If we scale z by $z' \equiv (c-a_l)z = 2\Omega_l s(1-\beta)z$, we then obtain

$$\Phi_{\alpha_l,\alpha_r} = \frac{s^{\alpha_p}\exp[-b+c]}{c}\,\Phi''_{\alpha_l,\alpha_r},$$

where $\Phi''_{\alpha_l,\alpha_r}$ is a function of β and $q_\perp^2$ only. Since we have $\alpha_p = 1$, $c \simeq$ $\simeq s(\Omega_l+\beta\Omega_r)$, and

$$-b+c \simeq 2(1-\beta)\Omega_l\left[m_1^2+\frac{\Omega_r}{\Omega_l+\beta\Omega_r}\mu^2\right]-\frac{2\Omega_l\Omega_r}{\Omega_l+\beta\Omega_r}q_\perp^2, \tag{4.10}$$

we immediately obtain this important «scaling» property: $\mathrm{d}\sigma/\mathrm{d}^4q\,\delta(q^2-\mu^2)$ is a function of only $q_\perp^2$ and $q_\parallel/q_{\max}$, in the region $q_\perp^2 = O((\text{mass})^2)$. Furthermore, the dominant $q_\perp^2$ dependence of $\Phi_{\alpha_l\alpha_r}$ will come from the exponential factor

$$\exp[-b+c] \propto \exp\left[-\frac{2\Omega_l\Omega_r}{\Omega_l+\beta\Omega_r}q_\perp^2\right].$$

The functional form of $\Omega_{\alpha_l\alpha_r}(q_\perp^2,\beta)$ (eq. (3.24)), in the case α_l, $\alpha_r = 0$ or $\frac{1}{2}$, is unfortunately not simple in the forward region. For the purpose of illustration, we shall consider the case $m_1^2 = \mu^2 = m_\pi^2$ and $q_\perp^2 = 0$, so that $\Omega_l m_\pi^2 \ll 1$ and therefore

$$|c-a_r| = 2\beta\Omega_l m_\pi^2\frac{[1-(\beta^2/(1-\beta))(\Omega_r/\Omega_l)(1+\Omega_r/\Omega_l)]}{1+\beta(\Omega_r/\Omega_l)} \ll 1.$$

Under this condition, the term $\exp[-(c-a_r)x]$ in eq. (4.3) can be approximated by unity, and for $\alpha_r = 0$, $\alpha_l = 0$,

$$\Phi_{00}\left(q_\perp^2, \frac{q_\parallel}{q_{\max}}\right) = \frac{\pi}{4\Omega_l(\Omega_l+\Omega_r)^2}\left(\frac{\beta^2}{1+\beta}\right)\gamma^2 F(\gamma), \tag{4.11}$$

where

$$F(\gamma) = \int_0^1 \mathrm{d}x \frac{x^2(1-x)}{1-\gamma x} = \frac{1}{\gamma^4}\left[\gamma\left(\frac{\gamma}{2} - 3\right) - (3-2\gamma)\log(1-\gamma)\right]$$

and

$$\gamma = \frac{(\Omega_l + \Omega_r)\beta}{\Omega_l + \Omega_r\beta}.$$

We now discuss the region where the end diagram may be important. The behavior of the end diagram in β is simply $\propto (s/M^2)^{2\alpha} \cdot (M^2)^{\alpha_P(0)} \propto \beta^{1-2\alpha}$, and it is immediately apparent from the rapid increase in the forward-production data with β that the end diagram is not important in most of this region. On the other hand, one can see that the central diagram, as in the example Φ_{00}, is a rapidly increasing function of β. The end diagram could only be of importance then for $\beta \approx 0$.

In general, one can show that $\Phi_{\alpha_l\alpha_r}$ behaves as $\beta^{4-2\alpha_r-2\alpha_l}$ as $\beta \to 0$. Consequently, the end diagram with a β dependence $\beta^{1-2\alpha}$, will dominate in most cases over the central diagram in the limit $\beta \to 0$, in agreement with our earlier assertion [6]. Then, as β increases, the central-diagram contribution will quickly take over, and increase very rapidly. Eventually, as $\beta \to 1$, we approach the pionization region and the distribution becomes independent of β. This indicates that in any production experiment, although the extremely energetic particles produced in the c.m. frame are mostly from the end diagrams, the greater portion of secondary particles arises from the central diagram.

5. – Summary.

In this paper we have examined the connection of the multi-Regge bootstrap model to the single-particle distribution spectrum [4-6,14]. We have concentrated on the contribution from the central diagram since the more direct but limited end diagrams have been covered in a previous paper [6]. The detailed calculation of the central diagram involved the integration of a simplified dynamical model over the momentum transfers to the clusters and over the subenergies of the clusters. Simplified forms of this result in particular kinematic limits have been given for illustration.

---

[14] Various averaged quantities related to momentum spectra have also been discussed by S. PINSKY and W. WEISBERGER: *Final state-spectra in a multiperipheral model*, Weizmann Institute preprint (to be published).

The general multiperipheral assumption of rapid damping in momentum transfer was shown to lead to characteristic properties of the single-particle distribution, which allow a classification of regions of single-particle phase space. The more specific assumption of the damped multi-Regge amplitude and its bootstrap results were used to obtain specific results for the distribution spectrum. Assuming the intercept of the Pomeranchuk trajectory to be unity, the spectrum was shown to possess the properties of pionization for small momentum in the c.m. and of scaling in longitudinal momentum in the forward- and backward-production regions. The illustrative results for various kinematic regions contain the damping and Regge-trajectory parameters of the multi-Regge amplitude in a way which would easily allow their determination and the parametrization of experiments.

We emphasize that while the single-particle distribution is one of the simplest inclusive experiments, its phenomenological analysis provides a fertile ground for parametrizing, testing and improving multiperipheral bootstrap models. Of special importance is the unified analysis of data in all of the kinematic regions. In addition, this general framework could be used to discover systematic differences between experiments involving different particles and trajectories.

* * *

It is a pleasure to thank M. L. GOLDBERGER for discussions.

APPENDIX

Central-diagram contribution to the single-particle distribution spectrum.

For the sake of generality, we shall express the contribution to the single-particle distribution spectrum coming from the central diagram in terms of the CGL auxiliary function B. This contribution can then be readily written in terms of the forward Reggeon-particle absorptive amplitude $\mathscr{A}$ through the use of eq. (2.8).

Consider a particular multiperipheral chain with N final particles. Let the detected particle in the central region of this chain have momentum q^μ and let us specify the multi-Regge amplitude T_N by a set of four-momentum transfers

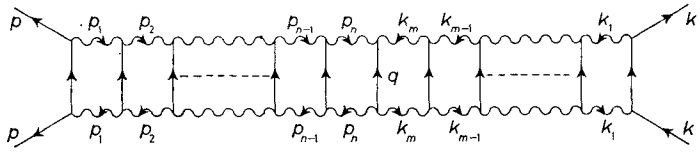

Fig. 7. – Central-diagram contribution to the single-particle cross-section.

to the left $\{p_i\}$, $1 \leqslant i \leqslant n$, and to the right $\{k_j\}$, $1 \leqslant j \leqslant m$, where $n+m+1=N$, as indicated in Fig. 7. The contribution to the total cross-section due to this N-particle intermediate state is

$$\sigma^N(p,k) = \frac{1}{2\Delta^{\frac{1}{2}}(s, m_1^2, m_2^2)} \int |T_N|^2 \, \mathrm{d}\Phi^N, \tag{A.1}$$

where the phase space $\mathrm{d}\Phi^N$ is ($p_0 = p$, $k_0 = k$)

$$\mathrm{d}\Phi^N(p,k;\{p_i\},\{k_i\}) = (2\pi)^4 \left\{\prod_{i=1}^{n} \frac{\mathrm{d}^4 p_i \, \delta^+((p_i - p_{i-1})^2 - \mu^2)}{(2\pi)^3}\right\} \cdot \left\{\frac{\delta^+((p_n + k_m)^2 - \mu^2)}{(2\pi)^3}\right\} \left\{\prod_{i=1}^{m} \frac{\mathrm{d}^4 k_i \, \delta^+((k_i - k_{i-1}) - \mu^2)}{(2\pi)^3}\right\}. \tag{A.2}$$

The contribution to the single-particle cross-section is

$$\mathrm{d}\sigma^N(p,k;q) = \mathrm{d}^4 q \, \frac{1}{2\Delta^{\frac{1}{2}}(s, m_1^2, m_2^2)} \sum_{\substack{n=1 \\ m=N-n-1}}^{N-2} \int |T_N|^2 \, \mathrm{d}\Phi^N \cdot \delta^4(q + p_n + k_m) \,. \tag{A.3}$$

The summation over n is due to the freedom of the location of the detected particle within the chain. The single-particle cross-section is then obtained by summing over N:

$$\mathrm{d}\sigma(p,k;q) = \sum_{N=3}^{\infty} \mathrm{d}\sigma^N(p,k;q) \,. \tag{A.4}$$

The summation over n and N can be converted to a sum over n and m and performed because of the factorizable nature of T_N and $\mathrm{d}\Phi^N$. Each sum over n and m leads to the presence of the CGL B-function. The N-particle phase space can be factored into a product of an n-particle and an m-particle phase space, with initial four-vectors (p, p_m) and (k, k_n) respectively:

$$\mathrm{d}\Phi^{N=n+m+1}(p,k;\{p_i\},\{k_j\}) = \mathrm{d}\Phi^n(p,p_n;\{p_i\}) \cdot \frac{\mathrm{d}^4 p_n \, \delta^+((p_n + k_m)^2 - \mu^2) \, \mathrm{d}^4 k_m}{(2\pi)^7} \, \mathrm{d}\Phi^m(k, k_n, \{k_j\}) \,. \tag{A.5}$$

Similarly the production amplitude can be factored into

$$T_{N=n+m+1}(p,k;\{p_i\},\{k_j\}) = = \frac{T_{n+1}(p,-k_m;\{p_i\})}{G(k_n^2)} \beta(p_n^2, \omega_{nm}, k_m^2) \frac{T_{m+1}(k,-p_n;\{k_j\})}{G(p_n^2)} \,, \tag{A.6}$$

where G is the single Regge coupling and β is the double Regge coupling. Substituting (A.5) and (A.6) into (A.2) and summing over n and m, one obtains

(replacing p_n, k_m by p', k'),

$$\text{(A.7)} \qquad \mathrm{d}\sigma(p, k; q) = \frac{\mathrm{d}^4q\,\delta^+(q^2-\mu^2)}{\Delta^{\frac{1}{2}}(s, m_1^2, m_2^2)}\,\frac{2}{(2\pi)^7}\sum_{n=1}^{\infty}\sum_{m=1}^{\infty}\int\left|\frac{T_{n+1}}{G}\right|^2|\beta|^2\left|\frac{T_{m+1}}{G}\right|^2 \cdot \frac{\mathrm{d}\Phi^m}{2}\,\frac{\mathrm{d}\Phi^n}{2}\,\mathrm{d}^4k'\,\mathrm{d}^4p'\,\delta^4(q+p'+k')\,.$$

Recalling that when B is integrated over it gives the absorptive part $(A - A_1)$ (eq. (2.6)), and that $A - A_1 = \Delta^{\frac{1}{2}}(s, m_1^2, m_2^2)\,\sigma_{\text{total}}$, we find from eq. (A.1) that

$$\text{(A.8)} \qquad B(-k', p'; p) = \tfrac{1}{2}\sum_{n=1}^{\infty}\int\left|\frac{T_{n+1}(p, -k'; \{p_i\})}{G(k'^2)}\right|^2\mathrm{d}\Phi^n(p, p'; \{p_i\})\,,$$

and

$$\text{(A.9)} \qquad B(-p', k'; k) = \tfrac{1}{2}\sum_{m=1}^{\infty}\int\left|\frac{T_{m+1}(k, -p'; \{k_j\})}{G(p'^2)}\right|^2\mathrm{d}\Phi^m(k, k'; \{k_j\})\,.$$

Using (A.8) and (A.9) in (A.7), we then obtain the single-particle spectrum in terms of the solution of the multi-Regge integral equations, eq. (2.9).

Note added in proofs. The derivations in this paper for the pionization region are valid not only for $q_\parallel \approx O(1)$ but for any $q_\parallel$ growing with s such that $q_\parallel/\sqrt{s} \to 0$ as $s \to \infty$.

Furthermore, considering the property of scaling, *i.e.*

$$\mathrm{d}\sigma/\mathrm{d}^4q\,\delta^+(q^2-\mu^2) = \Phi(2q_\parallel/\sqrt{s}, q_\perp)\,,$$

and the work of this paper showing Φ to be regular at $q_\parallel/\sqrt{s} \to 0$, we may expand Φ in a Taylor series about $q_\parallel/\sqrt{s} = 0$. For sufficiently small $2|q_\parallel|/\sqrt{s} < \varepsilon$, the first term in the series is dominant, giving $\Phi(2q_\parallel/\sqrt{s}, q_\perp) \simeq \Phi(0, q_\perp)$. Therefore the region of pionization extends up to the production regions of $2q_\parallel/\sqrt{s}$ fixed.

● RIASSUNTO (*)

Si sviluppa la relazione fra la dinamica multiperiferica e i relativi esperimenti ad alta energia. Si riportano le caratteristiche generali della distribuzione di singole particelle per i modelli multiperiferici con smorzamento esponenziale dell'impulso trasferito. Lavorando con un specifico modello di Regge multiplo si dimostrano inoltre i fenomeni di pionizzazione e di scala dell'impulso longitudinale per piccoli impulsi trasferiti. Si danno esempi degli spettri di distribuzione per valori specifici e fisicamente importanti dei parametri di Regge. Le predizioni possono servire come verifica per un modello realisitico per l'approccio con l'equazione integrale alla dinamica multiperiferica, e possono fornire una formula attendibile per parametrizzare i dati sperimentali.

(*) *Traduzione a cura della Redazione.*

Много-периферическая динамика и включающие эксперименты.

Резюме (*). — Выводится соотношение между много-периферической динамикой и включающими экспериментами при высоких энергиях. Выявляются общие особенности спектра распределения отдельной частицы для много-периферических моделей с экспоненциальным затуханием относительно передаваемого импульса. Работая со специальной множественной моделью Редже, мы, кроме того, отмечаем явления пионизации и подобия относительно продольного импульса для малых передаваемых импульсов. Приводятся примеры спектров распределения для специальных и физически важных значений параметров Редже. Эти предсказания могут служить как проверка реалистической модели для подхода на основе интегральных уравнений к много-периферической динамике, и могут обеспечивать разумную форму для параметризации экспериментальных данных.

(*) *Переведено редакцией.*